THE CENTRAL REGION OF THE PHILIPS AVF CYCLOTRON

P. Kramer, H.L. Hagedoorn and N.F. Verster
Philips Research Laboratories, Eindhoven
(Presented by P. Kramer)

The purpose of our study of central orbits in an AVF cyclotron is to get information about the horizontal motion, the phase with respect to the RF field, and the vertical-focusing properties of the central region.

As regards the horizontal motion, one wishes to know the position of the ion source such that the particles after several revolutions are situated within the stability triangle in phase space.

Furthermore, one is interested in the RF phase at which particles starting from the ion can be accelerated satisfactorily. For the vertical focusing one has to know the phase at which the particles cross the dee-dummy dee gap.

To improve the vertical focusing we started from the idea of Smith[1] to give the particles an increased path length in the dee during the first half revolution. From electrolytic tank measurements we found a source puller geometry giving a nearly homogeneous electric field between source and puller.

The horizontal motion, deduced from the measured electric field, was followed with both an analogue and a digital computer. In this way the orbits, their centres, and the phase of the particles were determined for different starting conditions.

The vertical motion was calculated by determining the focusing properties of the dee-dummy dee configuration. We started these computations from the beam shape as it was observed during an experiment in which we extracted the beam from the ion source with a d.c. voltage.

The Electric Field

The geometry of the cyclotron centre is shown in Fig. 1. The ion source is of the Livingston type[2]. Cathode and anticathode are placed in two chambers connected by a graphite chimney. The distance between dee and dummy dee is 2 cm and the diameter of the gap inside the dee is 25 mm. The puller is made of copper and has an inner gap of 6 mm. The ion source and puller shapes are designed to obtain a nearly homogeneous field with a 20^{0} angle to the dee. The graphite chimney of the ion source has an extension for this purpose. The distance between chimney and puller is 10 mm. The equipotential lines are shown in Fig. 1.

Calculations

The horizontal motion is described by the differential equations:

$$M\ddot{x} = eE_x(x, y)\cos\omega_e(t - t_o) - e\dot{y}B(x, y)$$
$$M\ddot{y} = eE_y(x, y)\cos\omega_e(t - t_o) + e\dot{x}B(x, y) , \qquad (1)$$

where: x and y are the coordinates parallel and perpendicular to the front of the dee; M and e are the mass and the charge of the particle; E_x and E_y are components of the electric field; and B(x, y) the magnetic field. We have assumed that $B(x, y) = B_o$.

We reduce the number of parameters as follows: (a) The RF frequency $\omega_e = eB/M$ by $\omega_e = (1 + \delta)\omega_o$, (b) we choose our time unit τ so that $\omega_o = 1$, (c) we represent the electric field by $E_x = F_x(x,y)V_D$ and $E_y = F_y(x,y)V_D$. V_D is the dee voltage and F_x, F_y are the components of the field in the model. We characterize the relation between V_D, B_o and e/M by the radius of curvature R of a particle with an energy eV_D in a field B. Substitution in Eq. (1) gives:

$$\ddot{x} = \tfrac{1}{2}R^2 F_x(x, y)\cos(1 + \delta)(\tau - \tau_o) - \dot{y}$$
$$\ddot{y} = \tfrac{1}{2}R^2 F_y(x, y)\cos(1 + \delta)(\tau - \tau_o) + \dot{x} \qquad (2)$$

We have solved these equations for R = 2, $2\sqrt{2}$ and 4 cm. R = 2 cm corresponds to 50 keV protons in a magnetic field of 15000 gauss.

The representation of the electric field depended on the computer we used. For the analogue machine (Pace, Electronic Associates) the main part of the field could be represented by an error function. The potential in the model V_m could be given by

$$V_m = \frac{1}{4\pi}\int e^{-\{y-y_o(x)\}^2 b(x)}\, dy \ .$$

The point of symmetry y_o and the steepness b(x) varied with x. To this part we added a correction for the asymmetry of the field occurring in the vicinity of the ion source.

This representation could be programmed in the machine. The machine plots the orbit (x, y) directly. A second plot gives $x - \dot{y}$ and $y + \dot{x}$, $\cos(1 + \delta)\tau$, and x as functions of τ ($y + \dot{x}$ and $x - \dot{y}$ are respectively the y and x coordinates of the orbit centre in the absence of an electric field).

The last plot is given in Fig. 2. The motion of the centre is clearly shown. The y-component of the electric field at the right side of the ion source, especially, gives an appreciable shift of the centre in the y-direction. This can be avoided by using a shorter puller. However, this will disturb the homogeneity of the field between chimney and puller.

In spite of the limited capacity for storing the electric field, the analogue

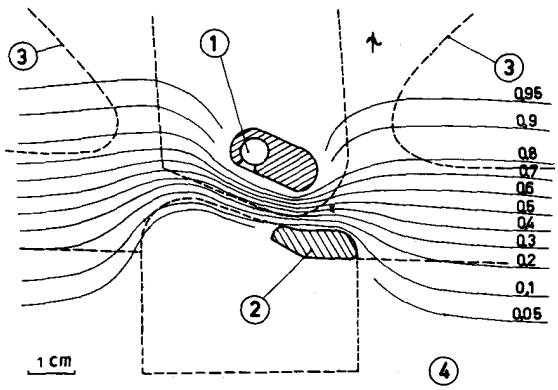

Fig. 1 Centre of the cyclotron with equipotential lines, measured in an electrolytic tank. 1) Ion source; 2) Puller; 3) Dummy dee; 4) Dee.

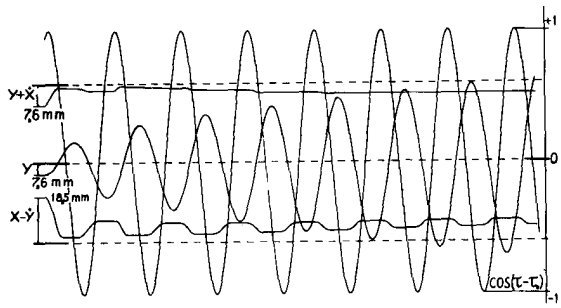

Fig. 2 Motion of the orbit centre during the first revolutions plotted with the analogue computer for a magnetic field of 15000 gauss and a maximum dee voltage of 50 kV.
a) x - y the abscissa of the centre.
b) y + x the ordinate of the centre.
c) y the ordinate of the particle.
d) cos ($\tau - \tau_0$).

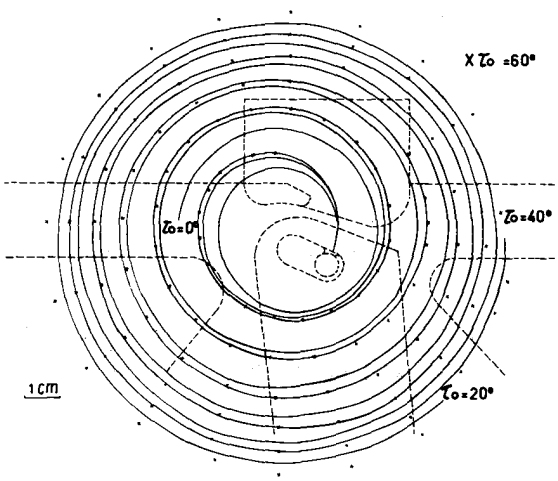

Fig. 3 First orbits for different starting phases calculated by digital computer Pascal.

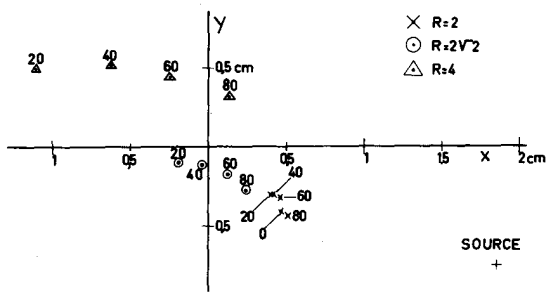

Fig. 4 Orbit centre after six revolutions for different starting conditions. R represents the radius of the first half revolution.

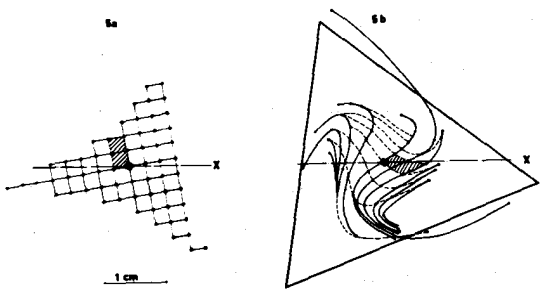

Fig. 5 a) A grid in phase space at the 6th revolution.
b) The same particles represented in phase space at the 50th revolution. The theoretical stability triangle is shown. The centre of the magnetic field is indicated by the small square.

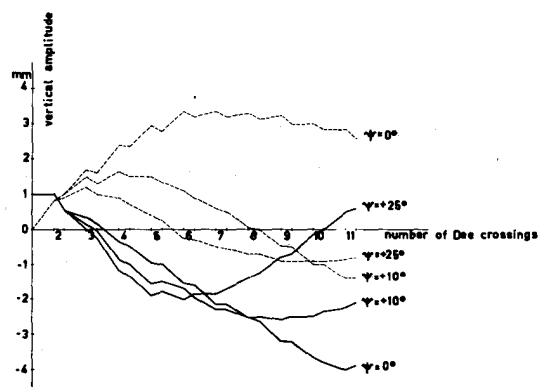

Fig. 7 Schematic diagram of the calculated vertical motion during the first revolutions. The full lines represent particles started 1 mm above the median plane in horizontal direction. The dotted lines represent the particles started in the median plane with a slope of 1%. ψ is the mean phase of the particles in the middle of the electrical lens system.

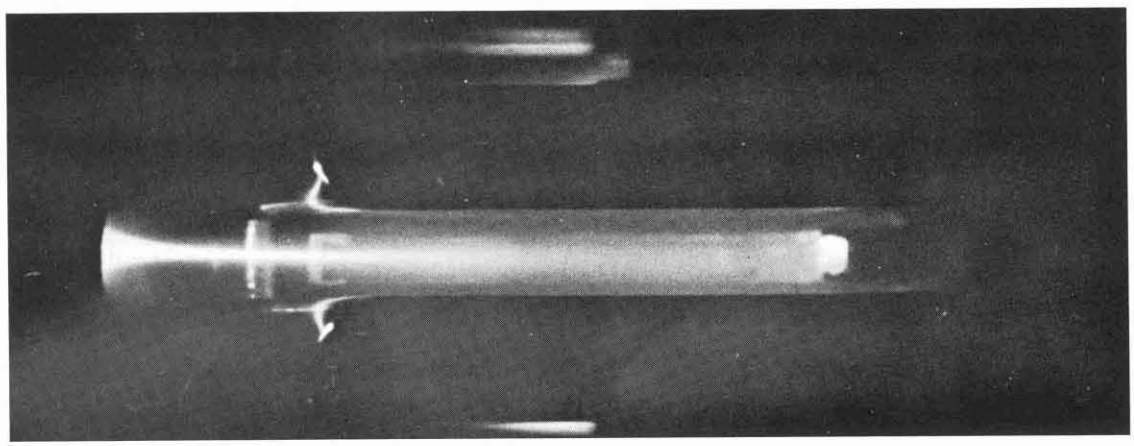

Fig. 6 The ion beam coming from the ion source. The d.c. voltage of the electrode is about 12 kV. The front of the electrode had the same shape as the puller.

computer is a rather accurate and convenient machine for solving the problem. The digital computer (Pascal, Philips) offers the possibility of extending the programme. We can introduce a magnetic field varying with x and y. However, we did not use this for the present calculations, since the influence of the flutter on the horizontal motion is very small in the centre.

The input of the electric field consisted of the y values of the equipotential lines at equidistant x values. From this the potential values are calculated in a square grid. In a square of this grid the potential is defined by $V = a + b\Delta x + c\Delta y + d\Delta x\Delta y$, where Δx, Δy are the coordinates in the square with respect to a corner. The sides of the squares were 2.5 mm.

The integration was performed by a second-order Runge-Kutta method. The accuracy was checked by variation of the step length. A higher order interpolation was considered to be useless with this representation of the electric field.

We made a number of computations for particles leaving the ion source with differing initial phases, and for differing values of R. Figure 3 gives orbits for R = 2 cm (50 keV protons, 15000 gauss) at starting phases 0, 20, 40, 60° ahead of the maximum in the RF voltage. The orbits do not spread appreciably so it is not possible to select particles of a particular phase with a vertical slit.

In Fig. 4 the orbit centres are shown after six revolutions for R = 2, $2\sqrt{2}$ and 4. For the x coordinate of the centre we took the average of the values at 6 and $5\frac{1}{2}$ revolutions. As has been shown[3], the deviations from the equilibrium orbit can be interpreted as a motion of the orbit centre. Using the analytical formulae following a method analogous to the one described in Ref. 4 the phase space after 6 revolutions has been transformed to that after 50 revolutions. The result is shown in Fig. 5. To obtain a beam, after 50 revolutions, lying well within the stability triangle and occupying a not too distorted area in phase space, the centre, after 6 revolutions, has to be situated about 5 mm from the centre of the magnetic field. Consequently, we have to move the ion source and puller combination if we alter the radius of the first half revolution R.

Vertical Motion

Since, in the centre of our cyclotron, neither the flutter nor the gradient guarantees magnetic beam focusing, the electric field has to produce sufficient focusing. In the appendix it is shown that the focusing properties of the electric field between the dee and the dummy dee can be represented by three lenses. The two outer lenses have opposite signs and are in general stronger than the inner one. The focal strengths of the two outer lenses are given by the formula:

$$\frac{1}{F_{out}} = \left(\frac{\Phi'}{4\Phi}\right)_{s=0}^{\cos(\psi)},$$

where Φ is the energy of the particle, Φ' is the increase of energy per unit of path length, and s is the coordinate of the path. s = 0 at the inner lens. ψ is the phase at s = 0. The inner lens has a strength

$$\frac{1}{F_{in}} = \int_{-}^{+} \frac{7}{16} \frac{\Phi'^2}{\Phi^2} \, ds + \frac{1}{2} \int_{-}^{+} \frac{\sin\psi}{r} \frac{\Phi'}{\Phi} \, ds \ ,$$

where r is the orbit radius. The integration extends over the whole electric field region for a dee crossing.

We calculated the vertical motion by determining the above mentioned parameters at the calculated horizontal orbits. After this we followed the motion by applying matrix multiplication.

We started from the shape of the beam as it was observed in an experiment with the ion source. We placed an electrode of the same shape as the puller in front of the ion source and extracted the beam from it with a negative voltage of about 15 kV. The result is shown in Fig. 6. The vertical dimension of the beam in the 6 mm puller gap is about 1 mm.

The results of the calculations are shown in Fig. 7. We started particles 1 mm above the median plane in the horizontal direction and other particles in the median plane but with a positive slope of 1%. Any other case can be deduced from these by linear combination. The focusing is sufficient for particles with an initial phase at the ion source of 0 - 60°. Particles starting at 80° will probably not be focused vertically. Particles at 0° hit the puller (Fig. 3). The appropriate starting phases lie between 10° and 60° and we can expect an acceleration of all these particles.

As can be seen in Fig. 7 an image of the initial beam cross-section is formed at a position depending on the starting phase. If we start a beam of small vertical dimension under a small angle within the median plane it is possible, by placing a horizontal diaphragm at the position of the focus for this particular phase, to select only a small phase region of the beam.

Appendix

If ν_z is the vertical oscillation frequency, ν_z^2 is a good measure for vertical focusing[5]. In the centre, however, this is not so, since the focusing is concentrated in small regions (dee gap) and varies strongly during the first revolutions.

For a numerical integration of the coupled motion one needs Φ'', for which our electrolytic tank measurements give strongly fluctuating values. Consequently, we sought another method and used matrix multiplication. We needed the strength and position of the lenses responsible for the vertical focusing.

We start from:

$$M \frac{d^2z}{dt^2} = - eF_z \ , \qquad (1)$$

where: z is the vertical coordinate and F_z the z component of the electrical field. We can evaluate F_z as

$$F_z = \frac{\partial F_x}{\partial x} z = z \cdot \frac{\partial^2 \Phi}{\partial x^2} + \ldots. \text{ (terms of order } z^3, z^5 \ldots\ldots\text{)}, \qquad (2)$$

where $\Phi = E + V$ = total energy of the particle. Neglecting higher order terms we get for Eq. (1)

$$M\frac{d^2z}{dt^2} + e\frac{\partial^2 \Phi}{\partial x^2} z = 0 \qquad (3)$$

We eliminate t as integration variable by

$$\frac{dx}{dt} = v = \sqrt{\frac{2e\Phi}{M}} \quad . \qquad (4)$$

Substitution in Eq. (3) gives

$$z'' + z' \frac{\Phi'}{2\Phi} + z \frac{1}{2\Phi} \frac{\partial^2 \Phi}{\partial x^2} \qquad (z' \text{ means } \frac{dz}{dx}). \qquad (5)$$

Now we can eliminate the z' term by the transformation

$$z = S\Phi^{-1/4} \qquad (6)$$

We now get an equation for S

$$S'' + \left(\frac{3}{16} \frac{\Phi'^2}{\Phi^2} - \frac{1}{4} \frac{\Phi''}{\Phi} + \frac{1}{2\Phi} \frac{\partial^2 \Phi}{\partial x^2}\right) S = 0 \quad , \qquad (7)$$

and introduce for V an a.c. voltage

$$V = V_0 \cos\omega(t - t_0) \quad . \qquad (8)$$

Particles cross the electric field when $\cos\omega(t - t_0) \sim 1$. By neglecting higher order terms we get, after substitution of Eq. (8):

$$S'' + \left(\frac{3}{16} \frac{\Phi'^2}{\Phi^2} + \frac{\Phi''}{4\Phi} + \frac{1}{2} \frac{\Phi'}{\Phi} \sin\psi \frac{1}{\omega} \sqrt{\frac{M}{2\Phi}}\right) S = 0 \quad . \qquad (9)$$

The variation of the vertical slope $\Delta S'$ is given by

$$\Delta S' = -\int_{-}^{+} \left(\frac{3}{16}\frac{\Phi'^2}{\Phi^2} + \frac{\Phi''}{4\Phi} + \frac{1}{2}\frac{\Phi'}{\Phi}\sin\psi\sqrt{\frac{M}{2\Phi}}\right) S\,dx = \frac{1}{f} S ,$$

where f is the strength of the lens needed for the matrix multiplication.

The first and third terms remain focusing during integration. Looking at the symmetry properties we can represent the effect of these two terms as that of one lens in the symmetry point of the electric field. The second term changes from focusing to defocusing and can be considered as the combination of two first order lenses of opposite signs and a second order lens in the middle. The big lenses are situated symmetrically with respect to the inner lens and the distance d between them is of the order of the dee gap

$$d = \frac{-\int_{-}^{+} \frac{\Phi'^2}{\Phi^2}\,ds}{\left(\frac{\Phi'^2}{\Phi^2}\right)_o} .$$

The second order part follows from integration of Eq. (9). It can be added to the lens corresponding to the first and third terms. The result is

$$\frac{1}{F_{out}} = \left(\frac{\Phi'}{4\Phi}\right)_{s=0} \cos\psi ,$$

$$\frac{1}{F_{in}} = \int_{-}^{+} \frac{7}{16}\frac{\Phi'^2}{\Phi^2}\,ds + \frac{1}{2}\int_{-}^{+} \frac{1}{\sin\psi}\frac{\Phi'}{\Phi}\frac{1}{\omega}\sqrt{\frac{M}{2\Phi}}\,ds .$$

References

1. W.I.B. Smith, Nucl. Instr. and Meth., 9, 49 (1960).
2. R.S. Livingston and R.J. Jones, Rev. Sci. Instr., 25, 552 (1954).
3. H.L. Hagedoorn and N.F. Verster, Nucl. Instr. and Meth., 18-19, 201 (1962).
4. H.L. Hagedoorn and N.F. Verster, Nucl. Instr. and Meth., 18-19, 336 (1962).
5. B.L. Cohen, Handbuch der Physik XLIV, page 105.

DISCUSSION

RESMINI : What is the accuracy of your electrolytic tank measurement?

KRAMER : I think it is 2%.

POWELL : In your plots it looks as if the electric field acting on the ion source slit would be rather weak. Did your d.c. experiment show any space charge effects?

KRAMER : Yes, we saw it. The width of the beam increased with output.

BLOSSER : Could you say at what current you began to see an expansion?

KRAMER : I think it was at about 1 to 2 mA d.c.

RESMINI : Did you in your vertical amplitude calculation take into account the radial variation of magnetic field?

KRAMER : No, not at all. Hagedorn made some calculations on that: if there is a focusing field it does not matter so much; in our case since we have a small flutter in the central region and a defocusing magnetic field it becomes rather worse.

RESMINI : So you have not used any magnetic coil in the centre?

KRAMER : No. The field here is strictly isochronous.